Journal of Intelligent Systems and Control
https://www.acadlore.com/journals/JISC

Advancements in the Design and Automation of Biomimetic Ornithopters: An Investigation into Flapping-Wing Flight Control

Adedotun Adetunla[1*], Bernard Adaramola[1], Habeebullah Abdulkadir[2]

[1] Department of Mechanical & Mechatronics Engineering, Afe Babalola University, 370001 Ado Ekiti, Nigeria
[2] Department of Aerospace Engineering, Iowa State University, 50011 Iowa, USA

* Correspondence: Adedotun Adetunla (adetunla.adedotun@abuad.edu.ng)

Received: 05-14-2023 **Revised:** 06-20-2023 **Accepted:** 06-25-2023

Citation: A. Adetunla, B. Adaramola, H. Abdulkadir, "Advancements in the design and automation of biomimetic ornithopters: An investigation into flapping-wing flight control," *J. Intell Syst. Control*, vol. 2, no. 2, pp. 99–109, 2023. https://doi.org/10.56578/jisc020204.

Abstract: Unmanned Aerial Vehicles (UAVs), in the form of ornithopters, which emulate avian flight through wing flapping, have been the focus of this investigation. The remarkable maneuverability of birds and insects, often lacking in conventional aircraft, is harnessed to advance the control and stability of flapping wing flight. The need for such exploration is driven by the potential benefits to both scientific inquiry and societal applications. This investigation tackles the task of tailoring the ornithopter's design and component choice to cater to performance expectations derived from the flight attributes of birds, such as superior maneuverability, agility, low-speed flight capabilities, and high propulsive efficiency. The primary goal is to ensure a sustained airborne state through the generation of lift equivalent to the ornithopter's weight. Commonly available materials have been employed in the construction of the ornithopter. SolidWorks flow simulator was utilized to simulate aerodynamics. A 1000mm length of the wing was subjected to a 3m/s air stream at a 5-degree angle of attack for the simulation. The simulated result, which represents a 2kg ornithopter, exhibited a lift force of 0.8N and a drag force of 0.2N. Further simulations were conducted at varying attack angles (from 0 to 35 degrees) to gauge the range of lift and drag coefficients. The investigation concludes that the constructed ornithopter should generate an upward thrust of 2.7N at a speed of 5m/s, even without wing flapping, ensuring controlled and stable flight.

Keywords: Flapping-wing flight; Aerodynamics simulation; Unmanned Aerial Vehicle; Wing mechanism; Electronic speed controller

1 Introduction

Ornithopters, Unmanned Aerial Vehicles with flapping wings, derive their name from the Greek words "ornithos", "meaning bird", and "pteron", meaning wing. These machines are designed to mimic the flight of birds and insects, operating on similar scales and employing similar forms [1]. The flapping mechanism within ornithopters transforms the rotational motion of motors through gears into the oscillating movement of wings, generating the lift and thrust required for flight. Functioning on principles comparable to airplanes, ornithopters produce lift by deflecting air downward as they move forward [2]. Instead of utilizing a rotating propeller, the wings of ornithopters flap, and various materials, including carbon fiber, plywood, and fabric, are used to construct wings that are both rigid and lightweight [3]. Unlike helicopters and fixed-wing aircraft, ornithopters employ oscillating or flapping airfoils rather than rotating ones, with the wings often serving the dual purpose of providing both lift and thrust [4].

Numerous attempts have been made to create ornithopters or robots that mimic wing-flapping motion [5, 6]. A notable early attempt occurred in 1060 when a monk glided approximately 200 yards before experiencing a non-fatal collision with the ground [7]. Later, Leonardo Da Vinci made significant advancements in ornithopter design, though his work was not thoroughly examined until the 19th century [7]. Da Vinci's investigations into avian flight led to the creation of a device wherein the pilot lays on a plank and operates large, membranous wings through hand levers, foot pedals, and a pulley system [8]. In 1871, Jobert's rubber band-powered model bird marked the conception of the first ornithopters capable of flight [9]. Later, rubber-powered ornithopters were produced by Cron et al., and Tatin's ornithopter introduced active wing torsion in the 1870s [10]. In 1890, Gustave Trouve developed the first internal combustion engine-powered ornithopter, which flew 70 meters during a demonstration for the French

Academy of Sciences [11]. Despite these advances, many designs failed to take off or achieve sustained flight due to their complexity or poor design.

The inability of most designs to generate sufficient lift for takeoff remains a significant challenge, preventing further research into areas such as maneuverability, flight distance, or time [12]. To maintain flight, the wings of an ornithopter must produce lift equal to its weight. Consequently, the development and selection of ornithopter components must consider performance requirements derived from the characteristics of bird flight, such as agility, low-speed flight capabilities, high propelling efficiency, and good maneuverability. Recent studies have managed to create micro aerial vehicles (MAVs) [13], flapping-wing micro aerial vehicles (FWMAVs) [14], and articulated ornithopters using a combination of two NACA airfoil series [15]. These studies identified propulsion efficiency and lift as crucial factors for ornithopter performance, with the flexibility of the outer portion of articulated wings contributing to improved propulsion efficiency, and the inner part providing lift. One study presented a schematic of an ornithopter with adequate flight stability and conducted an aerodynamic simulation using a SolidWorks flow simulator. The generated lift and drag forces were 0.8 N and 0.2 N, respectively, and the ornithopter developed in this study produced a 2.7 N upward thrust. These findings can serve as a benchmark for UAV manufacturers and expand the range of potential industrial applications for UAVs.

2 Methodology

The ability to achieve flight has always been present in nature. Birds, for instance, utilize principles of physical science to propel themselves through the air by flapping their wings and gliding over long distances. The balance of four fundamental forces—lift, propulsion, drag, and weight—allows for heavier-than-air flight in ornithopters. Figure 1 illustrates how these four forces directly influence the flight model. This section is divided into two subsections: Design and Fabrication, and Control System.

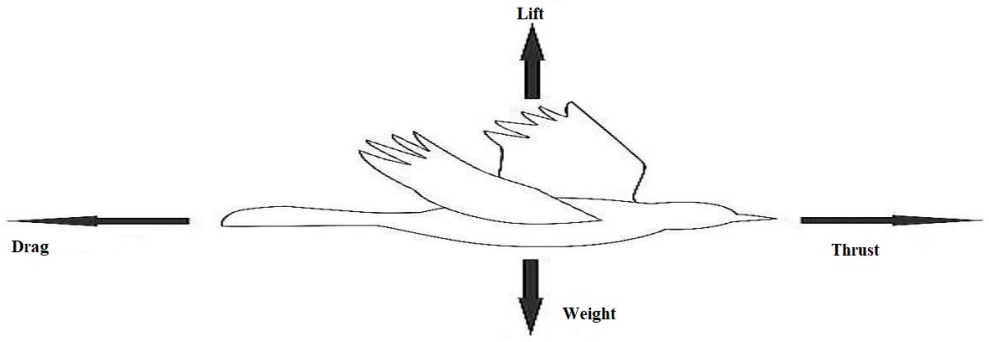

Figure 1. The four forces acting on a bird

2.1 Design and Fabrication

2.1.1 Material dimension

The materials selected for the ornithopter fuselage, its mechanical components, and their attachments were based on the following criteria: weight, strength, cost, fuselage frontal area, and shape. Material dimensions were considered as follows:

Wings: The most critical components of the model, affecting an ornithopter's flight characteristics, are its wings. A medium-sized ornithopter ranges from 30 cm to 2 m in size. In this study, the ornithopter's wingspan (b) was set at 124 cm, and the chord length (c) at 21 cm. An elliptical shape was chosen for the wing, with cotton material used for its construction. The wing area (S) was calculated using the following formula:

$$\text{Area of Wing } (S) = a \times b \times \pi$$

where,

$$a = \text{ wing span } \div 2 = 124 \div 2 = 62$$

$$b = \text{ root chord } \div 2 = 21 \div 2 = 10.5$$

$$\text{Wing Area } (S) = 62 \times 10.5 \times \pi = 2044.14 \text{ cm}^2$$

The aspect ratio and wing loading were carefully considered. The wing aspect ratio (AR), which determines a bird's maneuverability, is the ratio of the wing area (S) to the square of the wingspan (b).

$$AR = b^2/S = 124^2/2044.14 = 7.5$$

Higher wing loading requires a bird to fly faster to counteract the force of gravity (weight) [13]. The weight (W) of the intended model, including all electrical and mechanical components, was specified not to exceed 2 kg (2000 g). Wing loading is the ratio of weight (W) to wing area (S).

$$\text{Wing Loading } = W/S = 750/2044.14 = 0.387 \text{ g/cm}^2$$

The flapping frequency for the model was set to be between 2-5 Hz. Constants were established as follows:

- Coefficient of Drag (CD) = 2 (Based on airfoil type)
- Density of air = 1.225 kg/m^3
- Gravitational-induced acceleration (G) = 9.81 m/s^2
- Maximum angle the wing can make with regard to the body ($\boldsymbol{\theta}$) = 0.5236 radians

Subsequently, values were calculated and presented in Table 1:

- Drag force (Fd)

$$F_d = \rho \times C_d \times c \times b^3/3 = 1.225 \times 2 \times 0.21 \times 1.24^3/3 = 0.33 \text{ N}$$

- Angular Momentum ($\boldsymbol{\omega}$)

$$\omega = \sqrt{M} \times G/_{F_d} = \sqrt{0.75 \times 9.81/0.33} = 4.72 \text{rad/s}$$

- The time for the downstroke (T)

$$T = 1/(\omega \times \theta)^2 = 1/(4.72 \times 0.5236)^2 = 0.16s$$

- The torque (τ) of the wings

$$\tau = \rho \times \omega^2 \times C_d \times c \times b^4/8 = 1.225 \times 4.72^2 \times 2 \times 0.21 \times 1.24^2/8 = 3.4 \text{Nm}$$

- Power (P) in watts

$$P = \tau * \omega = 3.4 \times 4.72 = 16.04W$$

- Power (P_{hp}) in horsepower

$$P_{hp} = P * 0.00134102 = 16.04 \times 0.00134102 = 0.022$$

Table 1. Values of the ornithopter wing

$\mathbf{b(m)}$	$\mathbf{M(kg)}$	$\mathbf{c(m)}$	$\mathbf{F_d(N)}$	$\boldsymbol{\omega}\mathbf{(rad/s)}$	$\mathbf{T(s)}$	$\tau\mathbf{(Nm)}$	$\mathbf{P(W)}$	$\mathbf{P_{hp}}$
1.24	0.75	0.21	0.33	4.72	0.16	3.4	16.93	0.022

2.1.2 Material fabrication

The engineering drawings for the mechanical components of the ornithopter were created using SolidWorks, and the fabrication process adhered to these specifications, with minor dimension adjustments made as necessary.

•Fuselage and Gear Plates: The fuselage, being a critical component, required a design that was both lightweight and strong enough to withstand impacts [16]. A straw board template, scaled to the fuselage and gear plate drawings, was employed for fabrication. The casting mixture was introduced into a prepared acrylic mold and allowed to solidify. Once set, the cast was removed, cured on a level surface, and subsequently spray-painted, as depicted in Figure 2.

•Wings and Tail: The skeleton of the wings and tail was created using oxy electrodes, while aluminum sheets secured the electrodes in place for the tail. A cardboard template was employed to scale the wing drawing. The electrodes were then cleaned of carbon by hammering. The rods were connected by welding, and the wingtips were trimmed to match the marked pattern. As shown in Figure 3, the overall wingspan measures 1.234 m, with each wing possessing a surface area of 0.566 m^2.

•Flapping Mechanism: The shaft construction involved the use of two 8 cm-long cranks, a hollow aluminum rod, two circular wooden disks, and a plastic gear. These components were individually attached to the ornithopter during assembly, as illustrated in Figure 4.

•Wing Hinge and Holder: An iron steel metal sheet, measuring 12 cm by 4 cm, was cut and folded, leaving 4 cm on each edge for the wing hinge. After trimming the edges, ball bearings were positioned within the holes created by the oxy welding flame and secured using epoxy glue. As shown in Figure 5, two hinges were fabricated, and a wooden wing holder was constructed and fitted into the hinge.

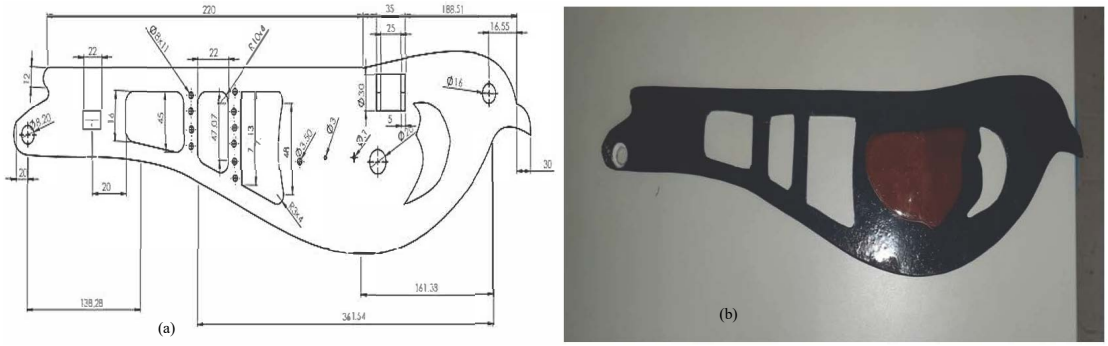

Figure 2. a: SolidWorks drawing of fuselage with dimensions; b: Finished fuselage and gear plates

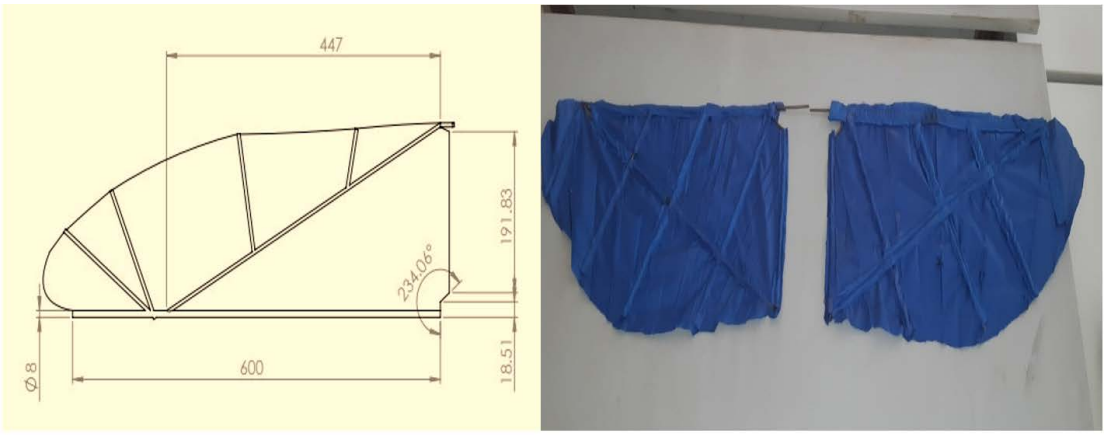

Figure 3. a: Dimensional SolidWork drawing of a wing; b: Competed wings

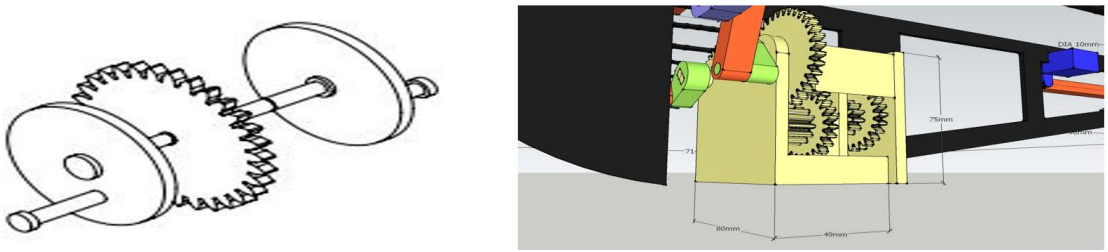

Figure 4. SolidWorks transverse transmission shaft isometric rendering

Figure 5. a: Housing of the wings; b: Completed hinge

2.2 Control System

The control system encompasses electronic controllers, motors, power sources, and electrical configurations, which collectively ensure the control and stability of the developed ornithopter.

2.2.1 Power source and motor

The model is powered by an A2212/13T Brushless Outrunner DC Motor. Generally, brushless motors exhibit an efficiency of 85–90%, while brushed DC motors have a 75–80% efficiency. Due to the increased efficiency, a greater proportion of the motor's total output is converted into rotational force, with less being lost as heat. This motor can draw a maximum current of 21.5A at 11.1V and has a 2200KV (rpm/v) rpm rating. It can provide up to 239W of maximum power when fully energized and reaches a rotation rate of 24,642 rpm when fully uncharged. Figure 6a demonstrates that the coil is stationary, while the outer magnet can rotate. The motor speed is controlled by a HK SS Series brushless 40A Electronic Speed Controller, as shown in Figure 6b, which delivers a continuous 30A and a 40A burst for 10 seconds. Lithium polymer batteries offer excellent energy storage to weight ratios in various forms and sizes [17]. The 25C 2200mAh 3S Lipo battery utilized is depicted in Figure 6c. The MC6 2.4GHz 6 channel transmitter and receiver control, illustrated in Figure 6d, provides exceptional performance, impressive range, and reliability. The microprocessor constantly searches for the optimal available channel to ensure worry-free flying without transmission issues.

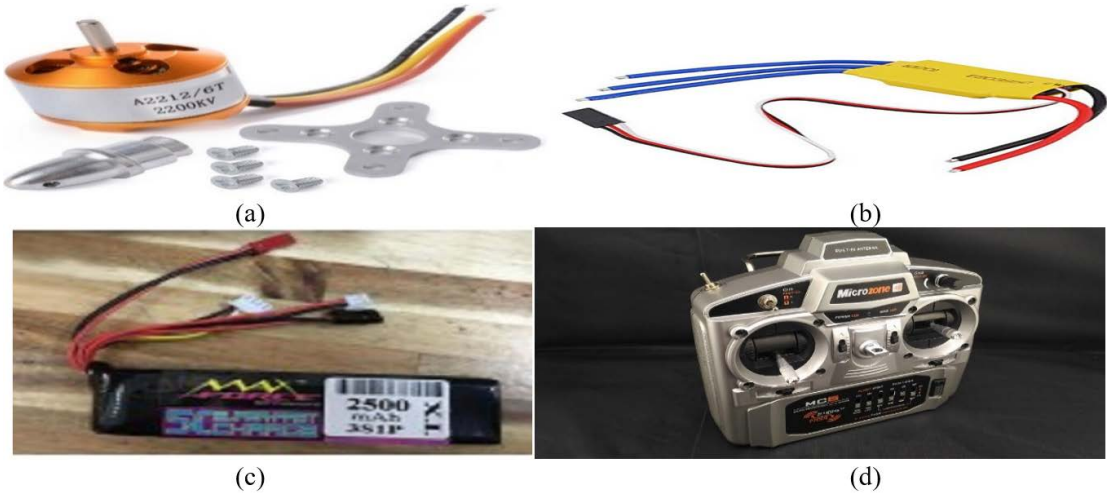

Figure 6. a: A2212/13T brushless outrunner motor; b: Electronic speed controller; c: 25C 2200mAh 3S Lipo battery; d: MC-6C 2.4GHz 6 channel transmitter and receiver

2.2.2 Electrical configuration and circuit

The electrical components (ESC and two servos) are connected to the RC receiver to enable control of the model's thrust, sideways, downward, and upward movement. A total of three channels are required for controlling the model bird. The two servos are connected to channels one and two of the receiver module, while the ESC is connected to the motor, which serves as the thrust channel of the receiver. The transmitter's high frequency results in a smaller antenna than an AM/FM transmitter and a null region in the direction of the antenna tip [18]. Consequently, it was ensured that the antenna tip would not face the model during flight for improved control. The ESC includes a battery-eliminating circuit that helps power both the receiver module and the servos. Additionally, a low voltage cut-off was incorporated to protect the Li-po battery from damage. The Raspberry Pi, equipped with Bluetooth and Wi-Fi, was utilized for streaming energy analysis data from sensors to a mobile device. The battery powers the receiver, which is also connected to the ESC, as shown in Figure 7, and directly connected to the servos for tail movement.

3 Results and Discussion

The aerodynamic behavior of various components of the ornithopter was investigated using Solidworks 2016's flow simulator. The assembled ornithopter is depicted in Figure 8, and the estimated weight is provided in Table 2.

3.1 Aerofoil Simulation

The aerodynamic behavior of the selected aerofoil, NACA741, was simulated and evaluated. NACA, the National Advisory Committee for Aeronautics, designates airfoils by series numbers. The three-digit NACA airfoil series was considered for this purpose, with each digit representing:

(1) Maximum camber as a percentage of the chord (first digit).
(2) Distance of maximum camber from the airfoil leading edge in tens of percent of the chord (second digit).
(3) Maximum thickness of the airfoil as a percentage of the chord (last digit).

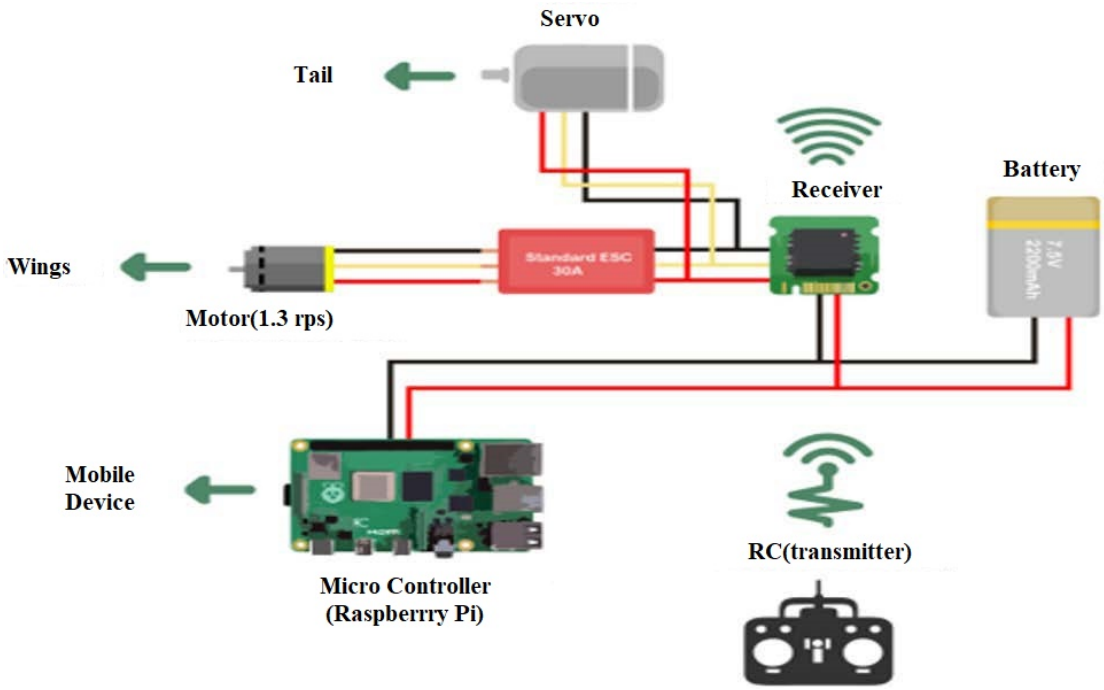

Figure 7. Connection of the model's hardware

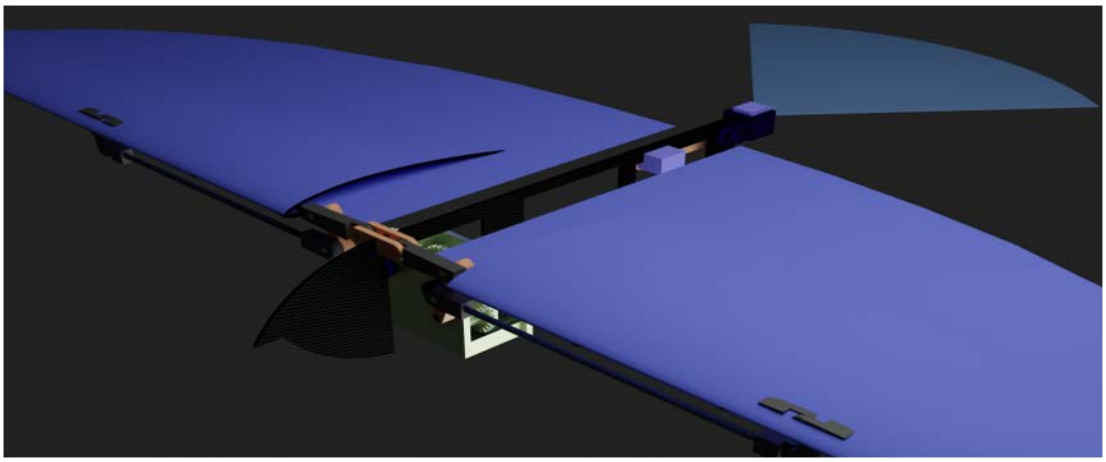

Figure 8. Coupling of various parts of the ornithopter

Table 2. Weight of the developed ornithopter

	Component	Mass (Kg)
1	Motor	0.156
2	Battery	0.386
3	Receiver & Transmitter	0.041
4	ESC	0.032
5	3 Servos	0.175
6	Fuselage	0.318
7	Wings	0.75
8	Gears & Fasteners	0.050
	Total	**1.91kg**

A study [19] found that the lift produced by the NACA741 airfoil surpasses that of the NACA0012 airfoil series, leading to the selection of NACA 741 for this investigation. A 1000mm length portion of the wing was placed in a 3m/s airstream at a 5-degree angle of attack for the simulation. The output data generated from the simulation are

presented in Table 3.

Table 3. Output data for aerodynamic simulations in aerofoil neutral position

Output	Unit	Value
Lift force	N	0.811
Drag force	N	0.200
Coefficient of lift		0.589
Coefficient of drag		0.145

The formation of lift requires that the air velocity profile above the aerofoil be greater than the velocity below the aerofoil, as illustrated in Figure 9.

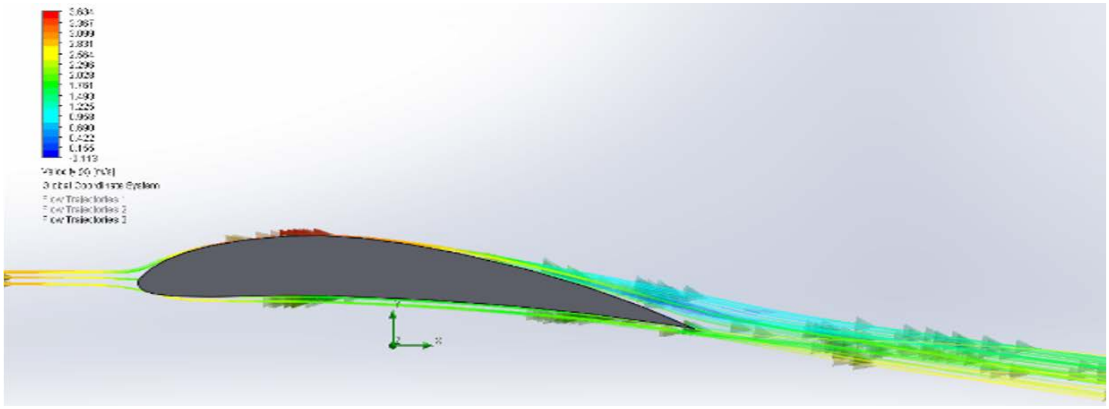

Figure 9. Simulated air flow around aerofoil section (velocity)

Another essential condition for lift generation is that the air pressure above the aerofoil is lower than the pressure below the aerofoil, as shown in Figure 10. Both criteria were met, leading to the incorporation of the aerofoil into the design. The NACA 741 airfoil generates a higher pressure difference around the airfoil compared to other airfoil series [20].

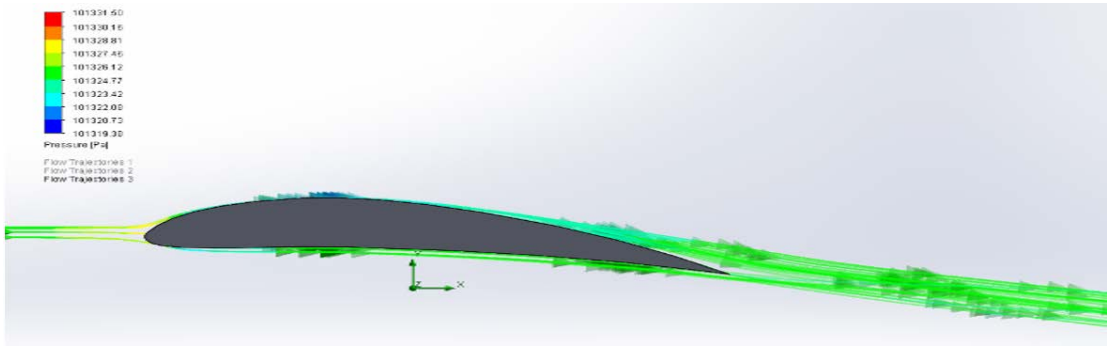

Figure 10. Simulated air flow around aerofoil section (pressure)

Simulations were performed for angles of attack ranging from 0 to 35 degrees. The data obtained from these simulations, presented in Table 4, were used to create the graphs in Figure 11, depicting the relationship between the Lift Coefficient, Drag Coefficient, and angle of attack, also known as the Lift and Drag Curve Slope.

This graph supports the choice of the aerofoil, as it has a higher slope compared to other aerofoils [21]. According to the simulation data, stalling occurs at an angle of 25 degrees, beyond which less lift is generated. The fluid flow trajectory at the stall point is shown in Figure 12.

3.2 Aerodynamics of the Ornithopter's Tail

The aerodynamics of the vertical stabilizer of the tail were investigated using Solidworks 2016 flow simulator. A 3D model of the ornithopter tail was accurately created and positioned in a 3 m/s airstream with a maximum angle of 15 degrees for the simulation. This simulation aimed to precisely calculate the drag and turning forces exerted by the wind on the tail. The results are presented in Table 5.

Table 4. Aerofoil aerodynamic simulation with varying angle of attack output data

Angle of attack (°)	Lift force (N)	Drag force (N)	Lift Coefficient	Drag Coefficient
0	0.354	0.146	0.257	0.106
5	0.811	0.2	0.589	0.145
10	1.158	0.31	0.84	0.225
15	1.49	0.435	1.082	0.316
20	1.421	0.838	1.03	0.608
25	2.009	0.872	1.458	0.633
30	1.727	1.136	1.253	0.824
35	1.567	1.505	1.137	1.092

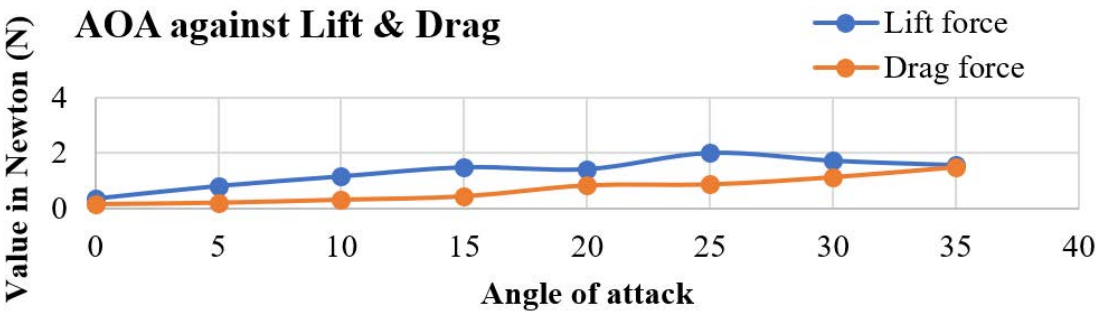

Figure 11. The relationship between lift, drag and angle of attack

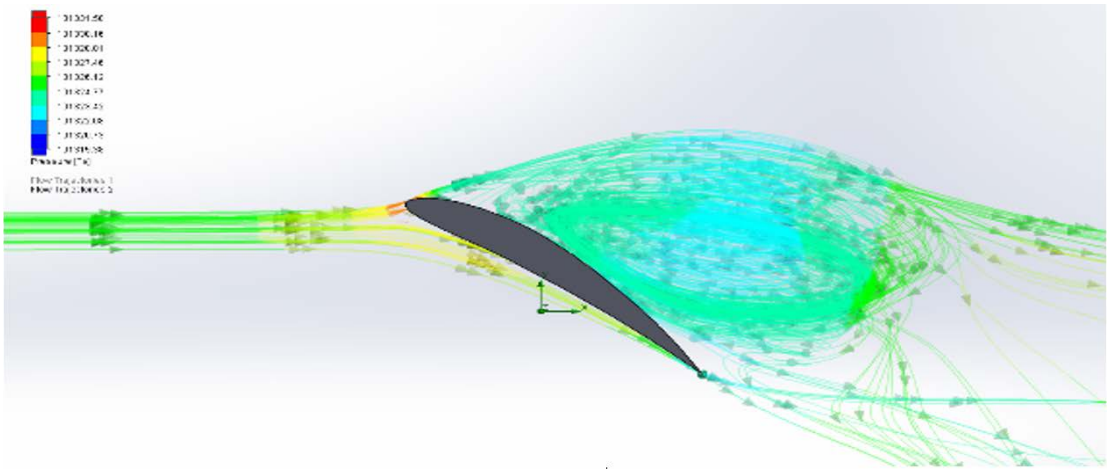

Figure 12. Aerofoil simulation at 25 degrees

Table 5. Output data from the tail aerodynamic simulation

Output (N)	Value	Minimum Value	Maximum Value	Averaged Value
Drag	0.029332741	0.029248855	0.030146473	0.029741314
Force (Y)	-0.088336854	-0.091534635	-0.088027001	-0.089962773

The negative sign of the forces indicates that they are pulling the tail in a downward, or negative Y, direction. Figure 13 illustrates the air flow path over the horizontal stabilizer of the tail.

3.3 Aerodynamic Simulation of the Ornithopter

Figure 14 displays the visual outcomes of the flow simulation for the ornithopter. A 3D model of the ornithopter was placed in a 5 m/s airstream with a 5-degree angle of attack for the simulation. The results generated by the simulation are shown in Table 6.

Based on the data, it is indicated that the ornithopter will be capable of generating 2.7 N of upward thrust at a speed of 5 m/s without the aid of flapping.

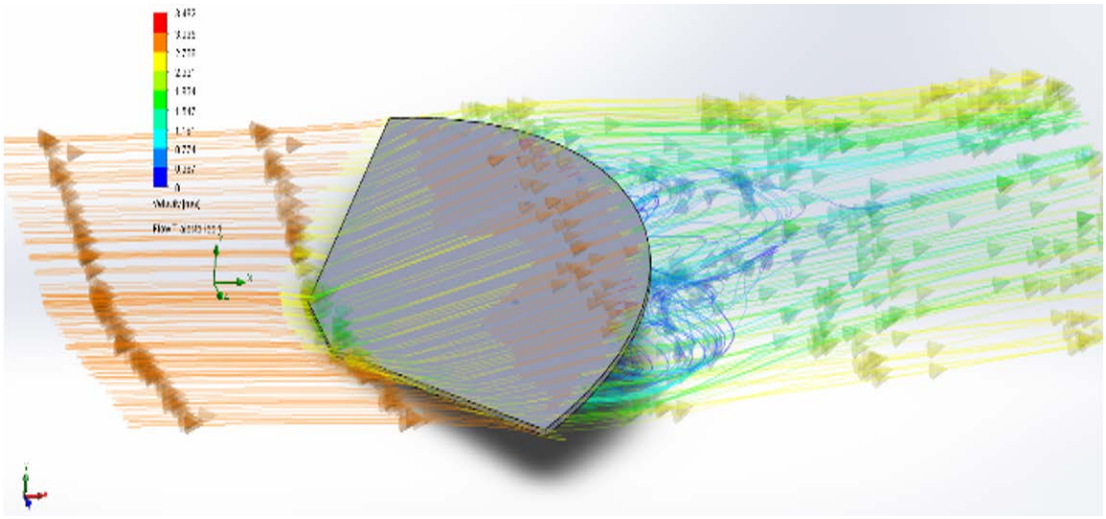

Figure 13. Aerodynamic simulation of horizontal stabilizer at 5 degrees

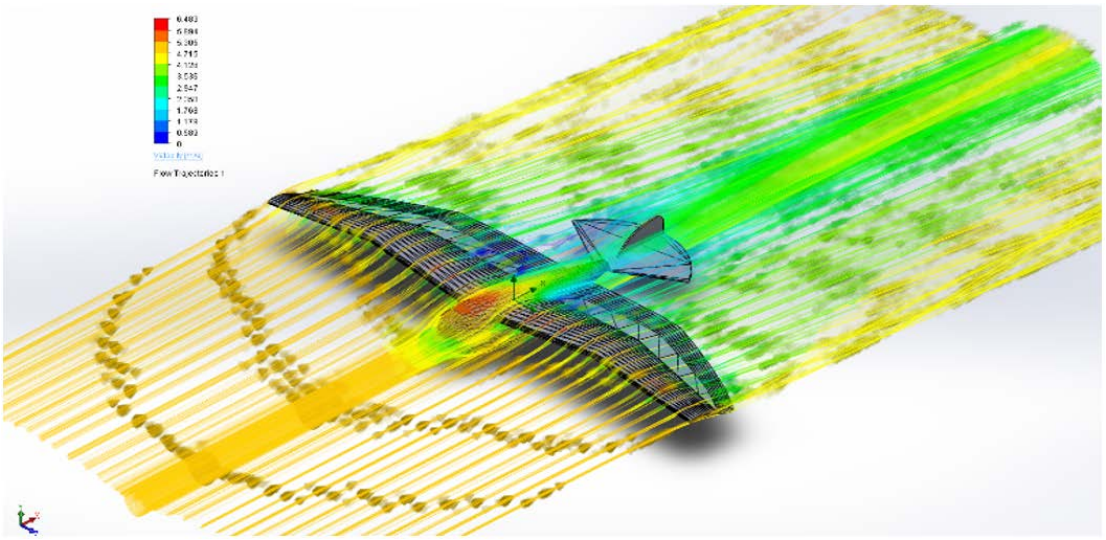

Figure 14. Aerodynamic simulation of ornithopter model

Table 6. Ornithopter aerodynamic simulation output data

Parameter	Value	Minimum Value	Maximum Value	Averaged Value
Drag Force (N)	0.601239474	0.599640774	0.604090165	0.60134382
Lift Force (N)	2.701223899	2.69085547	2.711809909	2.698637009
Lift Coefficient	1.960071763	1.952548187	1.967753222	1.958194655
Drag Coefficient	0.436273541	0.435113487	0.43834207	0.436349257

4 Conclusions

This paper has presented a comprehensive overview of the fundamental concepts underlying ornithopter design. In December 2004, the first ornithopter prototype was flown for less than a minute, weighing approximately 45 g and possessing a wingspan of about 40 cm. In this study, the size of the developed ornithopter was increased to 124 cm, and the weight was raised to approximately 2000 g, comparable to the typical weight of a bird. This allows for the possibility of flight in wind conditions greater than 5 m/s. It has been concluded that achieving successful, prolonged, and controlled flight presents numerous challenges. Firstly, a system similar to bird operation must be designed to improve flapping techniques. Secondly, an analysis of the ornithopter's aerodynamics is essential.

Through modeling and experimentation, the aerodynamic behavior of the developed ornithopter was characterized. It was found that the aerodynamic model used aligns well with experimental data in areas of high angle of attack and dynamic-stall effects without plunging motion. Other key findings include the mitigation of high flapping

frequency requirements by the long wingspan and the fact that the NACA 741 generates a higher-pressure difference around the airfoil compared to other studies. Moreover, the A2212/13T Brushless DC Motor was found to generate higher lift with the NACA 741 airfoil. This study concludes that the developed ornithopter will be able to generate 2.7 N of upward thrust at a speed of 5 m/s without the need for flapping wings, ensuring stable and controlled flight.

Funding

This study is self-sponsored research carried out at the Aerospace Laboratory of Afe Babalola University.

Data Availability

The data used to support the findings of this study are available from the corresponding author upon request.

Acknowledgements

The authors acknowledge the founder of Afe Babalola University, where this research was conducted.

Conflicts of Interest

The authors declare no conflict of interest.

References

[1] U. Rawat, A. Pawar, S. Roy, and R. Swami, "A designing approach for a flapping wing micro air," in *Proceedings of 7th IRAJ International Conference*, Pune, India, November 2013, pp. 7–13.

[2] I. Dubey and M. Amir, "A small unmanned flapping airvehicle 'ornithopter'," *Int. J. Sci. Eng. Res.*, vol. 8, no. 9, pp. 1256–1259, 2017.

[3] G. Singhal, "Unmanned aerial vehicle classification, applications and challenges: A review," *Preprints.org*, 2018.

[4] A. Bhargava and A. Bhargava, "Ornithopter design and operation," in *International Conference on Mechanical and Production Engineering*, Istanbul, Turkey, 2014, pp. 64–67. https://doi.org/10.1002/0470028505.ch7

[5] "Unmanned aerial vehicles: An overview," 2008. http://www.insidegnss.com

[6] S. Sharath, S. Kashyap, N. Subramanya, S. Kannur, and B. Vinod, "A review on bio-inspired ornithopter," *Int. J. Sci. Res. Dev.*, vol. 5, no. 5, pp. 474–479, 2017.

[7] G. Kumar, P. Kumar, S. Singh, and A. Reddy, "Design & analysis of ornithopter," *Int. J. Eng. Res. Afr.*, vol. 8, no. 3, pp. 217–226, 2020.

[8] S. Srigrarom and W. L. Chan, "Ornithopter type flapping wings for autonomous micro air vehicles," *Aerospace*, vol. 2, no. 2, pp. 235–278, 2015. https://doi.org/10.3390/aerospace2020235

[9] Z. J. Jackowski, "Design and construction of an autonomous ornithopter," Ph.D. dissertation, Massachusetts Institute of Technology, 2009.

[10] G. C. H. E. De Croon, M. A. Groen, C. De Wagter, B. Remes, R. Ruijsink, and B. W. Van Oudheusden, "Design, aerodynamics, and autonomy of the delfly," *Bioinspir. Biomim.*, vol. 7, no. 2, p. 025003, 2012. https://doi.org/10.1088/1748-3182/7/2/025003

[11] A. Bhargava, A. Bhargava, and S. K. Jangid, "Ornithopter development and operation," MAIET, Jaipur, India, Tech. Rep., 2015.

[12] I. Abel, "Design and feasibility study of personal ornithopters," Ph.D. dissertation, Swarthmore University, USA, 2014.

[13] A. Salmon, "Construction and operation," *Int. J. Mech. Eng. Res,*, vol. 6, no. 1, pp. 109–119, 2019.

[14] P. A. Force, S. Armanini, C. De Visser, and G. De Croon, "Data-informed quasi-steady aerodynamic model of a clap-and-fling flapping wing mav," in *International Conference on Unmanned Intelligent Systems (ICIUS)*, November 2015, pp. 1–6.

[15] S. Barve, A. Potdar, A. Kale, and P. Talekar, "Design and fabrication of an articulated ornithopter," *Int. Res. J. Eng. Technol.*, vol. 7, no. 10, pp. 755–759, 2020.

[16] M. Debiasi, Z. Lu, Q. V. Nguyen, and W. L. Chan, "Low-noise flapping wings with tensed membrane," *J. Aircr.*, vol. 58, no. 6, pp. 2388–2397, 2020. https://doi.org/10.2514/1.J058900

[17] V. Meiser, R. Henke, D. Šeatović, and M. Systems, "Autonomous unmanned ground vehicle as sensor carrier for agricultural survey tasks," in *International Conference of the European Society for Agricultural Engineers (EurAgEng)*, Zurich, Switzerland, July 6-10 2014, pp. 1–6.

[18] S. Akande, A. Adetunla, T. Olanrewaju, and A. Adeoye, "Uav and its approach in oil and gas pipeline leakage detection," *J. Robot.*, vol. 2021, pp. 1–12, 2021. https://doi.org/10.1155/2021/1300740

[19] G. R. Guntumadugu, “Design, development and operational of an ornithopter,” *Int. J. Innov. Res. Technol.*, vol. 6, no. 11, pp. 312–318, 2020.

[20] F. A. Vehicles, J. Han, Y. Han, H. Yang, S. Lee, and E. Lee, “A review of flapping mechanisms for avian-inspired,” *Aerospace*, vol. 10, no. 6, pp. 1–16, 2023.

[21] A. Adetunla and E. T. Akinlabi, *Finite Element Analysis of the Heat Generated during FSP of 1100 Al Alloy*. Springer, 2019, pp. 425–431. https://doi.org/10.1007/978-981-15-5753-8_39